Promoting Uranium Immobilization by the Activities of Microbial Phosphatases

Patricia Sobecky[1], Robert J. Martinez[1], Melanie J. Beazley[2] and Martial Taillefert[2]

[1]School of Biology, Georgia Institute of Technology, Atlanta Georgia and [2]School of Earth and Atmospheric Sciences, Georgia Institute of Technology, Atlanta Georgia

Abstract

The goal of this project is to examine the role of nonspecific phosphohydrolases in naturally occurring subsurface microorganisms for the purpose of promoting the immobilization of radionuclides through the production of phosphate precipitates. This project will focus on uranium (U), a radionuclide that poses significant risk to human health and the environment. Nonspecific acid phosphohydrolases are a broad group of secreted microbial phosphatases that function in acidic-to-neutral pH ranges and utilize a wide variety of organophosphoester substrates. We hypothesize that subsurface microorganisms that exhibit (acid) phosphatase activity and are resistant to heavy metals have the potential to immobilize U via a biomineralization process. Biomineralization, defined as the immobilization of an element by non-redox microbial precipitation, could prove to be a feasible alternative or complementing remediation approach to U bioreduction and adsorption processes. The primary objective is to demonstrate that the intrinsic phosphatase activities of indigenous subsurface microbes result in the release/accumulation of sufficient PO_4^{3-} to cause the formation and precipitation of low solubility U-phosphate minerals in oxygenated groundwater and soil. A three-step experimental approach is being conducted to examine the relationship between the occurrence of microbial phosphatases and metal resistance among the DOE Field Research Center (FRC) strains we are currently studying along with the contribution of LGT in the dissemination of these beneficial phosphatase genes. Our preliminary testing of a subset of FRC isolates cultured from contaminated FRC soils and background (reference) soils indicate a higher percentage of isolates exhibiting phosphatase phenotypes (i.e., in particular those we surmise to be PO_4^{3-}-irrepressible) relative to isolates from the background reference site. A high percentage of strains exhibiting such putatively PO_4^{3-}-irrepressible phosphatase phenotypes were also shown to be resistant to lead as well as cadmium. We have designed PCR primer sets for amplification of class A, B and C acid phosphatases from the FRC subsurface isolates.

Hypotheses to be tested:

(1). Non-specific phosphohydrolases (acid phosphatases) provide subsurface microorganisms with resistance to heavy metals and lateral gene transfer has promoted the dissemination of this phosphatase-mediated resistance.

(2). Phosphatase activities of the subsurface bacterial populations can promote the immobilization of radionuclides via the formation of insoluble metal phosphate precipitates.

(3). Subsurface geochemical parameters (pH, nitrate) will affect phosphate mineral formation by altering microbial phosphatase activity and/or affecting the stability of the metal phosphate precipitates.

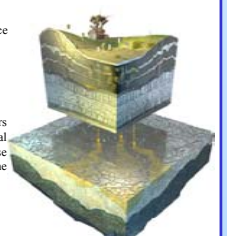

Image from: http://www.inel.gov/initiatives/subsurface.shtml

Figure 1. Map of U.S. Department of Energy-NABIR Field Research Center in Oak Ridge, TN from which sediment cores from contaminated Areas 1, 2 and 3 were sampled on February 18-24, 2003. Sediment cores from the background area (not shown) were obtained during the same sampling period.
Figure from http://public.ornl.gov/images/FigureA4.jpg

Figure 2. Lead [Pb(II)] resistance screening of FRC isolates from Areas 1, 2, 3 and the reference background site. Isolates cultured from Area 3 exhibited the highest incidence (61%) of Pb(II) resistance relative to Areas 1, 2 and the background site.

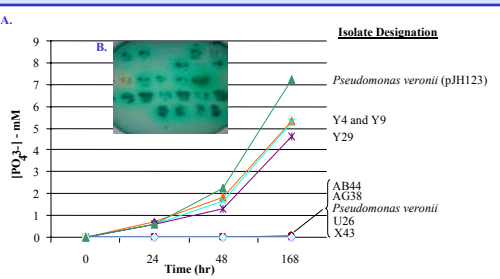

Figure 3. (A) Phosphate liberation of select FRC isolates which were identified as Pb[r] and exhibiting cell surface and/or extracellular phosphatase activity. FRC isolates assayed for phosphate liberation were obtained from the background reference site (AG38), Area 2 (AB44) and Area 3 (U26, X43, Y4, Y9 and Y29). A subsurface *Pseudomonas veronii* V1 isolate from Subsurface Microbial Culture Collection (SMCC) harboring the constitutive phoA plasmid pJH123 and the plasmid free *Pseudomonas veronii* V1 host were used as positive and negative controls for phosphatase activity, respectively. **(B)** Tryptose Phosphate Methyl Green (TPMG) agar plates were used to screen for phosphatase phenotypes. Phosphatase positive phenotypes appear as dark green colonies and/or cause the surrounding medium to darken. Negative phenotypes appear unstained.

A.

H. influenzae napA [Y07615]	TTTGATATTGATGATACCGT-••-TAATGCGTGCCGCAAACTC
S. enterica aphA [AJ237788]	TTTGATATTGACGACACCGT-••-TCCTGCGCGCGGCTAACTC
S. typhimurium aphA [AY125468]	TTTGATATTGACGACACCGT-••-TCCTGCGCGCGGCTAACTC
E. coli MG1655 *aphA* [X86971]	TTTGATATCGATGACACGGT-••-TTCTGCGCGCCTCCAACTC
M. morganii napA [X78328]	TTTGATATTGACGACACTGT-••-TATTACGCGCTTCGAACTC
Consensus Sequence	TTTGATAT--GA-GA--AC---GT-••-T--T----CG--GC---C---AACTC

Primers Designed Forward Primer 5'-TTTGATATYGAYGAYACBGT-3'
Reverse Primer 5'-GAGTTNGMVGCRCGYADDA-3'

Figure 4. (A) Alignment of a highly conserved domain of prototypical class B acid phosphatases. A similar approach has been used to design PCR strategies to amplify class A and class C phosphatases (data not shown). **(B)** Results of PCR strategy using genomic DNA from *E. coli* MG1655 and primers we have designed to amplify class B acid phosphatases. The final product is a 451-bp DNA fragment that is sequenced. Gel lanes: 1) size ladder (bp); 2) negative control; 3) positive template control; *E. coli* MG1655 16S rDNA amplicon (~1425 bp) used to verify amplification efficiency of genomic DNA template; 4) class B phosphatase amplicon amplified with PCR primers designed for this study

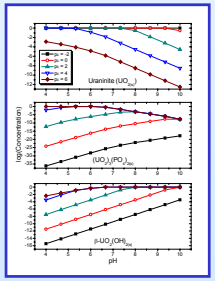

Figure 5. Concentrations of uraninite and the prevalent uranium phosphate and uranium hydroxide minerals found at equilibrium as a function of pH and pε in a typical contaminated groundwater containing U_T = 50 µM; ΣPO_4^{3-} = 40 µM; ΣCO_3^{2-} = 500 µM. At log (Concentration) = 0, the mineral precipitates. Dissolved uranium is essentially non-existent at pH < 7 at all pεs. At high pε and high pH, a maximum of 10% is found in solution as an $UO_2(HPO_4)_2^{2-}$ complex. From these calculations, low pH and high pε favor precipitation of uranium phosphate, high pH and low pε favor precipitation of uranium hydroxides, while a low pε favors precipitation of uraninite.

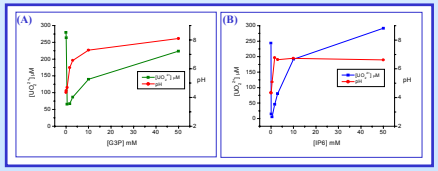

Figure 6A-6B. Solubility of U(VI) as a function of **(A)** G3P and **(B)** IP6 after 24 hour abiotic equilibration. Solubility of U(VI) in G3P decreases sharply between 0.1 and 0.5 mM G3P and then increases at high concentrations. U(VI) is highly insoluble at low concentrations of IP6 and precipitates completely. At higher concentrations of IP6 the solubility of U(VI) is enhanced, possibly due to increased repulsive negative charges around the uranyl ion. U(VI) analysis by laser-induced fluorescence (LIF) with pyrophosphate/hypophosphite reagent. Excitation at 395 nm and emission at 500 nm. Minimum detection limit 0.5 to 2 µM depending on medium. Sample solutions contain 300 µM uranyl acetate and 10 mM glycerol in a basal salts media (BSM). IP6 was added in a 1.6:3.4 ratio of phytic acid:Na-phytic acid to provide a slightly acidic solution.

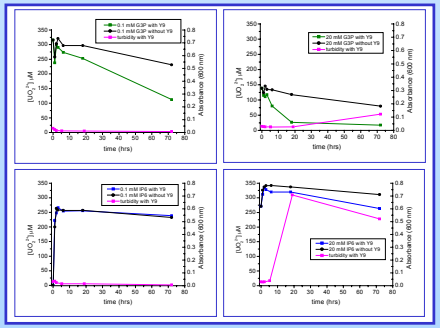

Figure 7A-7B. Kinetic study of U(VI) bioprecipitation in solutions containing isolate Y9 with G3P and IP6 as phosphate sources. All solutions contained 10 mM glycerol as a carbon source and 300 µM uranyl acetate in BSM medium. Samples were equilibrated for 24 hours and filtered (0.2 µM pore size) before adding Y9. At time 0, Y9 was added and the samples incubated for 72 hours at 30°C. Control samples without Y9 demonstrate the abiotic precipitation of U(VI). **(A)** After 72 hours in 0.1 mM G3P, 37.7% more U(VI) was precipitated biologically compared to the chemical control. **(B)** In 20 mM G3P, 87.5% of U(VI) was precipitated in the Y9 sample and 42.5% abiotically removed in the control, resulting in a 45.0% increase in biotic precipitation. **(C)** Due to 100% abiotic precipitation at time 0 in the 0.1 mM IP6 samples, a second amendment of 300 µM uranyl acetate was needed. After 72 hours, only 12% U(VI) was precipitated with little difference between the biotic and abiotic samples, indicating most of the IP6 had been removed prior to addition of Y9. **(D)** In 20 mM IP6, 17.5% more U(VI) was precipitated biologically compared to the abiotic control. U(VI) was least soluble in 20 mM G3P **(B)** and 0.1 mM IP6 **(C)** with 54% and 100% abiotic precipitation, respectively, before adding Y9.

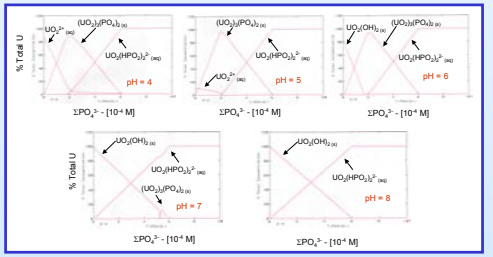

Figure 8. U(VI)-phosphate speciation at equilibrium predicted by MINEQL+ as a function of phosphate concentration in solution and pH . At low pH and low phosphate concentration, uranium is mainly under the form of uranyl ions. As the concentration of phosphate approaches that of total uranium, highly insoluble uranium phosphate compounds are formed. In excess phosphate, speciation calculations predict dissolution of this mineral and formation of uranium phosphate complexes in solution. At higher pH, uranium tends to be insoluble at low concentration of phosphate and soluble, as uranium phosphate complexes, at high phosphate concentration. The solid phase preferentially formed at pH > 7 is a uranium hydroxide mineral. These calculations were performed in the absence of carbonate species to illustrate the effect of phosphate on uranium speciation. Addition of carbonate does not change the behavior of uranium and phosphate.

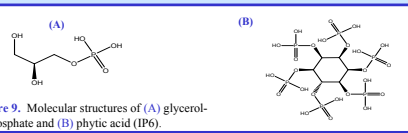

Figure 9. Molecular structures of **(A)** glycerol-3-phosphate and **(B)** phytic acid (IP6).

Conclusions and Future Directions

• Biomineralization may be complementary to bioreduction in the immobilization of uranium from contaminated sites. The objective of this study was to determine if the phosphatase activity of subsurface microbes results in the release of sufficient PO_4^{3-} to complex and precipitate UO_2^{2+}.

•Preliminary testing of a subset of lead-resistant subsurface isolates indicate a higher percentage of strains exhibiting phosphatase phenotypes from contaminated soils relative to isolates obtained from uncontaminated soils.

•To date, the majority of the lead-resistant, phosphatase positive isolates obtained from the FRC contaminated soils are Gram-positive *Bacillus* and *Arthrobacter* species. Enrichment cultures, using phytic acid and other phosphatase substrates, will be developed to obtain additional Gram-positive and Gram-negative isolates.

•Future studies will include the molecular characterizations of non-specific acid phosphatases from select FRC isolates will be conducted to determine substrate range, enzyme activity, optimal pH and the specific class (i.e., class A, B or C) using PCR primer sets developed in this project.

• Kinetic studies were conducted in solutions containing the Y9 isolate and an organo-phosphate compound to determine if the phosphatase activity of Y9 would enhance the precipitation of uranium (Figure 7).

•For these incubations two organo-phosphate compounds with different chemical structures were chosen as the phosphate source to determine how efficiently Y9 can hydrolyze these compounds. Phytic acid (IP6) is a six-member carbon ring with six attached orthophosphate groups which can provide up to twelve coordinate binding sites. Glycerol-3-phosphate is probably a more labile compound with only one orthophosphate attached to a three carbon chain. At neutral pH both molecules are negatively charged providing reactive sites for cationic binding.

•Studies were run at low (0.1 mM) and high (20 mM) concentrations of IP6 and G3P to account for the fact that abiotic precipitation of UO_2^{2+} is highly dependent on the concentration of these organo-phosphate compounds in solution (Figure 6). The solubility of UO_2^{2+} increases significantly with IP6 concentration. At high concentrations of IP6 the repulsive negative charges of the phosphate oxygens may hinder the ability of the phosphate complexes to nucleate and precipitate (Figure 8), therefore increasing solubility. U(VI) demonstrates high solubility at the lowest concentration of G3P, a sharp decrease in solubility as G3P content is increased up to 0.5 mM, followed by an increase in solubility at high G3P concentration.

•The solubility of U(VI) in the presence of Y9 followed the results shown in Figure 7. After 72 hours at both concentrations of G3P there was 38 to 45% enhancement of U(VI) precipitation in the biotic assays compared to the chemical controls. Suggesting U(VI)-phosphate mineral bioprecipitation. The IP6 assays had little difference between the control and the biotic sample. After 72 hours there did appear to be a slight enhancement of U(VI) precipitation of 17% in the biotic assay possibly indicating a longer time needed for bioprecipitation to occur with less-labile compounds.

•The results of this study provide positive indications that the removal of U(VI) from contaminated systems may be significantly enhanced through microbial enzymatic processes. Further study is needed to determine the speciation of the U(VI) complexes and the solid phase formed, and to assess the optimal environmental conditions needed for maximum uranium biomineralization in the subsurface.

Acknowledgements

This research is supported by the Office of Science (BER), U.S. Department of Energy, Grant No. DE-FG02-04ER63906